Dynamic properties of proton transfer in hydrogen-bonded molecular systems

2000 J. Phys.: Condens. Matter 12 885

(http://iopscience.iop.org/0953-8984/12/6/312)

J. Phys.: Condens. Matter **12** (2000) 885–906. Printed in the UK PII: S0953-8984(00)97423-X

Dynamic properties of proton transfer in hydrogen-bonded molecular systems

Xiao-feng Pang†‡ and H J W Müller-Kirsten†

† Department of Physics, University of Kaiserslautern, D-67653 Kaiserslautern, Germany
‡ Institute of High-Energy Electronics, University of Electronic Science and Technology of China, Chengdu 610054, People's Republic of China

E-mail: pangxf@mail.sc.cninfo.net.de and mueller1@physik.uni-kl.de

Received 10 September 1998, in final form 6 April 1999

Abstract. The mechanism of the formation of ionic and bonding defects and the interaction between protons and heavy ions in hydrogen-bonded molecular systems is investigated and a new model is constructed. This model considers two coupled sublattices corresponding to those of protons and heavy ions in order to study the dynamic properties resulting from deformation and local fluctuation of the heavy ion sublattice due to the protonic displacements. As compared with other models, the model emphasizes, in particular, the collective effect of the motion and the mutual correlation between the two sublattices. The equations of motion admit analytic soliton solutions of different types corresponding to two different defects. The combined effect of the two defects and the proton transfer in the system are described by means of these solutions, and the appropriate conditions associated with actual physical processes. Finally, we discuss in detail the characteristics of the proton transfer and the advantages of the model.

1. Introduction and presentation of physical background

It is well known that hydrogen-bonded chains consisting of a series of hydrogen bonds occur in many condensed matters and living systems, such as, for example, ice, solid alcohol, carbon hydrates and proteins. The understanding of proton transfer in hydrogen-bonded systems, which exhibit a considerable electrical conductivity even though electron transfer through the systems is hardly supported, is a long-standing problem. New ideas from nonlinear dynamics and soliton motion have provided a possibility to find an answer to this issue [1, 2]. This investigation becomes even more important in view of the close connection with the problem of proton transfer across biological membranes, which is something that could explain some fundamental properties of life [3–5].

In the case of studies of proton transfer processes in hydrogen-bonded systems, for example in ice, water or proteins, it is usual to consider one-dimensional chains, so-called Bernal–Fowler filaments [6, 7]. In the normal state of a chain each proton is linked to a heavy ion (or oxygen atom in ice) by a covalent bond in one case, or a hydrogen bond in the other. Therefore, there are two kinds of arrangements of hydrogen bonded states in these systems, namely the type X–H $\cdots$ X–H $\cdots$ X–H $\cdots$ X–H $\cdots$ X–H and the type H–X $\cdots$ H–X $\cdots$ H–X $\cdots$ H–X $\cdots$ H–X. Obviously the two states should have the same energy. In such a case it is accepted that the potential energy of the proton should have the form of a double well with two minima corresponding to the two equilibrium positions of a proton between two neighbouring heavy

0953-8984/00/060885+22$30.00

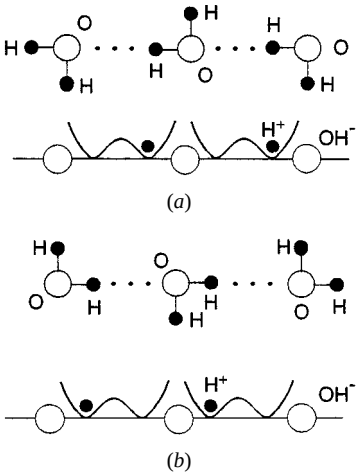

Figure 1. The double-well potential in the hydrogen-bonded system with H^+ in one well (*a*) or the other (*b*) of the potential.

ions (or oxygen atoms) as shown in figure 1. The barrier which separates them has a height which is in general of the order of the oscillation energy in a covalent bond X–H and is approximately 20 times larger than that in a hydrogen bond. In the usual case, the protons in the hydrogen bonds are subject to harmonic vibration with small amplitudes about their equilibrium positions.

When the protons in the system are perturbed by an externally applied field, light or energy is released, for example by ATP hydrolysis in protein molecules. Then localized fluctuations of the protons appear, and the states and positions of the protons change. The protons then move and deviate from their equilibrium positions, for instance by a translation, a jump, a shift or by migration in the interbonds and intrabonds. This phenomenon of proton transfer along hydrogen-bonded chains is observed experimentally, the protonic conductivity along the chain being about 10^3–10^4 times larger than that in the perpendicular direction. The motion of the protons may result in the ionic and bonding (orientational or Bjerrum) defects which correspond to the exchange and rotation of bonds, respectively [8–12]. Thus the transfer of protons along the hydrogen-bonded chain is caused by the transport of the two types of defects as shown in figures 2 and 3. It is possible that protons are transferred by jumps from one water molecule to another along the hydrogen-bonded chain, and that a migration of hydroxonium and hydroxyl ionic defects takes place in the intrabonds. However, when a proton approaches a molecule occupying a boundary of the chain, it may form a covalent bond, for example in ice with the oxygen atom of the molecule and then the original proton moves to a neighbouring molecule. When this process is repeated we have a transfer of the proton along the chain. The chain thus changes its state and the transfer of the proton is not possible in the same direction. The latter can be achieved only if a re-orientation of OH groups takes place by the second defect mechanism: the Bjerrum defect. The motion of an orientation defect contains simple successive rotations of OH groups, starting at one end of the chain and ending at the other. As a result of these rotations the creation of a pair of D and L defects moving to different ends can take place in any internal part of the chain. A sequence of rotations of all of the molecules in a filament returns the chain to its original state. It follows that the motion of another proton can occur only after the passage of a Bjerrum defect. In figure 4 we show a potential model of a positive bonding defect for such systems.

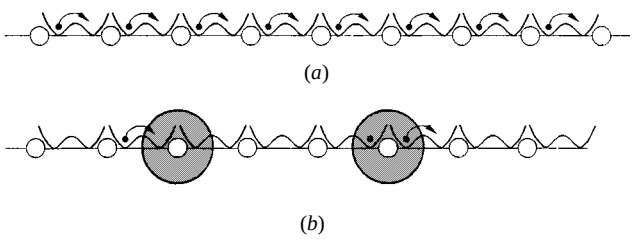

(*a*)

(*b*)

Figure 2. The two ionic defects in the hydrogen-bonded system.

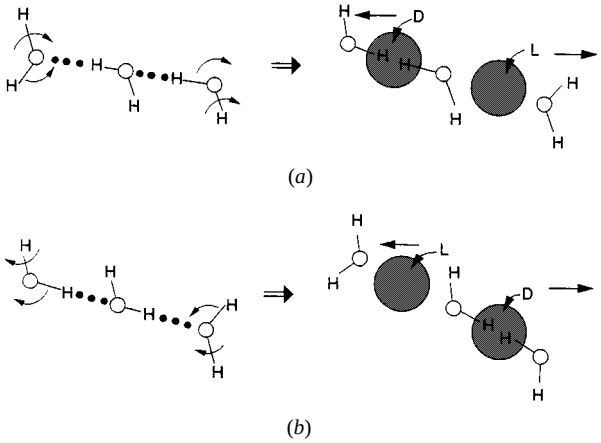

(*a*)

(*b*)

Figure 3. The two Bjerrum defects in the hydrogen-bonded system.

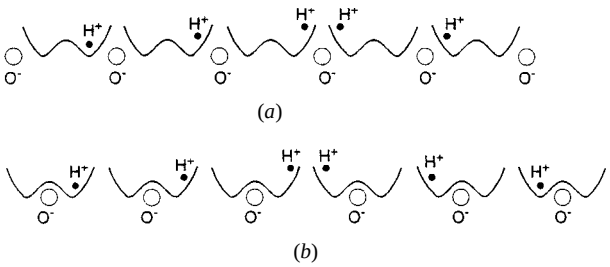

(*a*)

(*b*)

Figure 4. The model with double-well potential curves for the two types of defect.

The soliton model of proton transfer was first proposed by V Ya Antonchenke, A S Davydov and A V Zolotaryuk (the ADZ model) [1]. Further investigations have given solutions for a far greater range of velocities [2, 14]. The problem was further pursued in a number of papers [15–27] in which a variety of theoretical extensions—involving also Pnevmatikos *et al*'s [35] one-component protonic chain with a new two-parameter, double periodic, on-site potential—have been achieved. The basic idea of the ADZ model is that the coupling between the oxygen atoms and protons have only one mechanism to reduce the height of the barrier which protons have to overcome to pass from one molecule to another. This is included in this model by coupling the proton motion with an optical mode of the heavy ionic sublattice. The nature of this sublattice depends on the systems we study. In this model an ionic defect appears as a kink or solitary wave in the proton sublattice, propagating together with a localized contraction of the relative distance between neighbouring oxygens.

This excitation is referred to as a two-component solitary wave. In this model the proton potential with the double-well ansatz plays an essential role in the description of the motion of ion defects as topological solitary waves, the nonlinear interaction generated by the coupling between the protons and oxygen atoms playing only a secondary role by reducing the height of the barrier. Therefore, the properties of the solitons are mainly determined by the double-well potential. Thus this model is only effective for explaining the transfer of ion defects. The model's equations are also very difficult to solve, so that no exact analytical solutions can be given. Furthermore, if realistic values for the parameters of hydrogen-bonded systems are considered, the continuum approximation fails due to the narrowing of the domains of validity of the solutions with respect to the lattice spacing. This is the case in ice in which the H_3O^+ or OH^- ions become almost point defects. It is also very difficult to accept the one-component model of [14, 15] because the influence of the heavy ionic sublattice on the protons in their model was not considered in detail, and in our opinion, this is not very reasonable. Therefore, the proton transfer in the hydrogen-bonded systems is still an open problem. A complete theoretical description of the combined effect of the transfers of both types of defects has not been given so far. Thus, it is very desirable to improve and develop previous models by introducing new ideas and methods.

On the basis of a renewed analysis of the mechanism forming the two defects, we here propose a new model to study the dynamic properties of proton transfer resulting from the localized fluctuations of the protons and the deformation of the structure of the heavy ionic sublattice due to the displacement of the protons. The model emphasizes, in particular, the collective effects of the protons, and the correlation interaction between the two sublattices. Our Hamiltonian not only considers the change of the relative positions of neighbouring heavy ions arising from the motion of the proton, but also their interaction, including the dipole–dipole interaction and the resonant interaction between neighbouring protons. Thus we get some new results due to the difference of this model with previous models. An advantage of this model is that it admits analytic soliton solutions in a continuum approximation. Utilizing these solutions we can explain the motions of the two types of defects, and the proton transfer in the hydrogen-bonded system. Our study could also be extended in other related directions, but this will be the aim of future investigations.

The paper is organized as follows. In section 2 we construct the model and propose the model Hamiltonian of the system. In section 3 we derive the equations of motion and give the corresponding soliton solutions in a continuum approximation. In section 4 we investigate the elementary properties of the solitons. The system potential is examined in section 5. Finally section 6 discusses the results and the advantages of this model.

2. Construction of the model and the Hamiltonian of the system

In the model we consider that the hydrogen-bonded chain consists of two interacting sublattices of harmonically coupled protons (of mass m) and heavy ions (hydroxyl groups for ice, or complex negative ions, of mass M) as shown in figure 5. Each proton lies between a pair of heavy ions, usually referred to as 'oxygens'. The proton is connected by one covalent bond and one hydrogen bond with the two neighbouring oxygens. Therefore the potential energy of the proton in each hydrogen bond has the form of a double-well potential with the two minima corresponding to the two equilibrium positions of the proton. Obviously the double-well potential is motivated, physically, by the simultaneous electromagnetic interaction of the two neighbouring oxygens with the proton. When the proton can cross over the central barrier of the double-well potential from one well to the other, the relative positions of the proton and the two neighbouring oxygens have changed, and the positions of the covalent and hydrogen

bonds have also exchanged. Thus the ionic defects occur in the system as described in the usual models. In such a case the position of the proton in the hydrogen bond is mainly determined by the double-well potential. The proton displacement is controlled by the elastic interaction involved in the model. The coupling interaction between the proton and the oxygens can only play a complementary role, which reduces the height of the barrier the proton has to overcome to pass from one well to another, and thereby facilitates the proton crossover in view of the weaker coupling between the proton and the oxygens and the long distance between them. However, when the proton approaches the neighbouring oxygen the coupling interaction between the proton and oxygen will be greatly enhanced in the intrinsically nonlinear system. Thus the relative position between the proton and the oxygen will also be greatly changed, i.e. the migration of the proton as well as the deformation of the heavy ion sublattice by stretching and compression are enhanced. This phenomenon may result in the change of the direction of the covalent bond between the proton and the oxygen, i.e. the rotation of the bond. In fact, as far as the covalent bond is concerned, the so-called rotation of the bond in chemistry is simply carried out by the relative displacements of the proton and the oxygens with charges. Thus the Bjerrum defect occurs due to the coupling interaction in this intrinsically nonlinear system as shown in figure 6. Evidently the crossovers of the protons or the rotations of the bonds are mainly determined by the coupling interaction between the protons and the oxygens. Therefore the mechanism forming this defect is different from that of the above ionic defect, although they are all produced due to the changes of the relative positions of the protons and oxygens. For the protons in our model we assume an electromagnetic interaction between the neighbouring protons, including the dipole–dipole interaction and resonant interaction, except for the above double-well potential and the elastic interaction caused by the covalent interaction and related actions. Thus, it is also natural to take into account the changes of the relative positions of the neighbouring heavy ions resulting from this interaction. Assuming again, for the heavy ionic sublattice, the harmonic model with acoustic vibrations of low frequency, the Hamiltonian of the system can be written as

$$H = H_p + H_{ion} + H_{int} \tag{1}$$

where

$$H_p = \sum_n \left(\frac{1}{2m} p_n^2 + \frac{1}{2} m\omega_0^2 R_n^2 - \frac{1}{2} m\omega_1^2 R_n R_{n+1} + U(R_n) \right) \tag{2}$$

and

$$U(R_n) = U_0 \left[1 - \left(\frac{R_n}{R_0} \right)^2 \right]^2 \tag{3}$$

$$H_{ion} = \sum_n \left(\frac{1}{2M} P_n^2 + \frac{1}{2} \beta (u_n - u_{n-1})^2 \right) \tag{4}$$

$$H_{int} = \sum_n \left(\frac{1}{2} \chi_1 m (u_{n+1} - u_{n-1}) R_n^2 + m \chi_2 (u_{n+1} - u_n) R_n R_{n+1} \right) \tag{5}$$

where the proton displacements and momenta are R_n and $p_n = m\dot{R}_n$ respectively; the first being the displacement of the hydrogen atom from the middle of the bond between the nth and the $(n + 1)$th heavy ions or OH's in the static case. R_0 is the distance between the central maximum and one of the minima of the double well. U_0 is the height of the potential barrier. Similarly u_n and $P_n = M\dot{u}_n$ are the displacement of the heavy ion from its equilibrium position and its conjugate momentum respectively. Furthermore $\chi_1 = \partial\omega_0^2/\partial u_n$ and $\chi_2 = \partial\omega_1^2/\partial u_n$ are coupling constants between the protons and the heavy ion sublattice, which represent the changes in the energy of vibration of the protons and of the coupling energy between

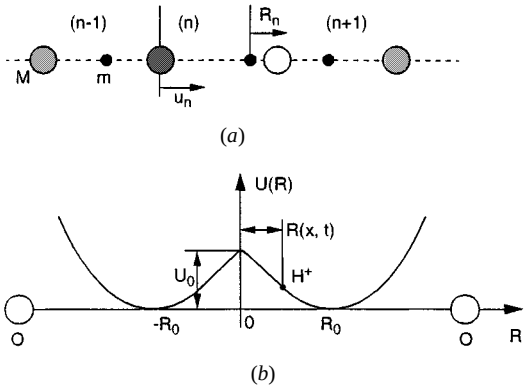

Figure 5. The one-dimensional lattice model for a hydrogen-bonded quasi-diatomic chain.

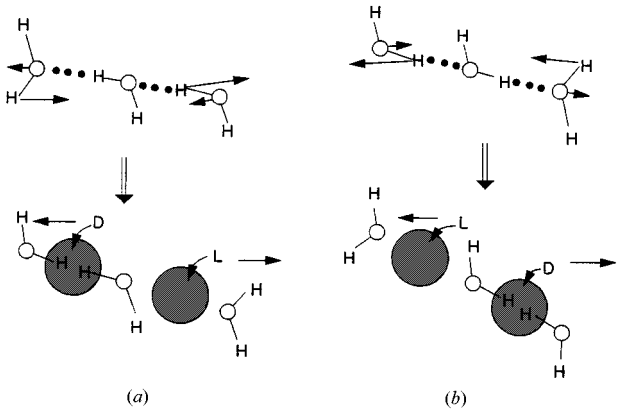

Figure 6. Schematic models each with a Bjerrum defect in the hydrogen-bonded system.

neighbouring protons due to the unit extension of the heavy ion sublattice, respectively. The quantity ω_0 is the frequency of harmonic vibrations of the protonic sublattice. The quantity $\frac{1}{2}m\omega_1^2 R_n R_{n+1}$ shows the correlation interaction between neighbouring protons caused by the dipole–dipole interactions. ω_0 and ω_1 are diagonal and non-diagonal elements of the dynamical matrix of the proton respectively. The quantity β is the linear elastic constant of the heavy ionic sublattice. m and M are the masses of the proton and heavy ion respectively. $C_0 = u_0(\beta/M)^{1/2}$ is the velocity of sound in the heavy ionic sublattice, and u_0 is the lattice constant. The part H_p of H is the Hamiltonian of the protonic sublattice with an on-site double-well potential $U(R)$, H_{ion} being the Hamiltonian of the heavy ionic sublattice with low-frequency harmonic vibration and H_{int} is the interaction Hamiltonian between the protonic and the heavy ionic sublattices.

From the above Hamiltonian, equations (1)–(5), we see that the new model is still a coupled model of two oscillators (proton and heavy ion) which is similar with the ADZ model [1, 2]. However, the former is significantly different from the latter for the following reasons. (i) So far as state and motion of the heavy ion in our model is concerned, it is only a harmonic oscillator with low-frequency acoustic-vibration, due to large mass containing a great number of atoms or atomic groups. However, the heavy ion has both acoustic and optical vibrations in the ADZ model, the physical idea, which is rather vague, we think is because the optical

and acoustic vibrations are two different forms of vibration in nature. Therefore, we think that our model for the heavy ion is more appropriate than the ADZ model. (ii) As far as state and motion of the proton lying in the double-well potential is concerned, we here adopted a model of a harmonic oscillator with optical vibration that includes a non-diagonal factor, which comes from the interaction between neighbouring protons, and interaction with the heavy ions; namely its vibrational frequencies are related to displacements of the heavy ions, which shows the coupled interaction between the protonic and heavy ionic sublattices, thus we can approximately obtain

$$\omega_0^2(u_n) \approx \omega_0^2 + \frac{\partial \omega_0^2}{\partial u_n}(u_n - u_{n-1}) = \omega_0^2 + \chi_1(u_n - u_{n-1})$$

$$\omega_1^2(u_n) \approx \omega_1^2 + \frac{\partial \omega_1^2}{\partial u_n}(u_n - u_{n-1}) = \omega_1^2 + \chi_2(u_n - u_{n-1}).$$

By inserting the above formulae into the protonic Hamiltonian and again taking into account the neighbouring heavy ions in left- and right-hand sides of the proton we naturally get to (2) and (5). Therefore our Hamiltonian has high symmetry and a one-to-one corresponding relation. However the ADZ's Hamiltonian does not. As a matter of fact, the vibration of the proton is acoustic, which is contrary to the heavy ion in the ADZ model. This is not reasonable for the protonic model, we think, because the vibration frequency of the proton is very high relative to the heavy ion due to its small mass and the strong interaction accepted. Therefore our model of the proton is more appropriate than that of the ADZ model. Moreover, the relation between the protonic and interactional Hamiltonians in the ADZ model does not have a one-to-one correspondence, as mentioned above in our model. Moreover the physical meaning of the interaction Hamiltonian is also very vague or difficult to understand in the ADZ model. Thus the ADZ model cannot give a strictly analytic solution at all, so we do not know what are the real properties and the law of the proton transfer in the systems in the ADZ model!

As far as our model Hamiltonian is concerned, not only is the physical idea very clear and easily understandable, but it also has high symmetry and one-to-one correspondence between H_p and H_{int}. It completely and exactly represents the dynamic features and states of the proton and heavy ion and the interactions between them occurring in the systems when compared with the ADZ model and other models [1, 2, 13–19, 23–28]. In fact, the above Hamiltonian in our model not only includes the optical vibration of the protons, but also the resonant interaction caused by the electromagnetic interactions between neighbouring protons, and it also takes into account both the change of the relative displacement of the neighbouring heavy ions resulting from the vibration of the proton and the correlation interaction between the neighbouring protons. These facts clearly show that our model is new and expresses the properties of the systems. Therefore, our model is more appropriate than the ADZ model. Thus we can expect that our model can reveal some new results when compared with the ADZ model or other models.

3. The equations of motion and their soliton solutions

With Hamilton's equations (cf [38–43]) we obtain from (1)–(5)

$$\dot{p}_n = -\frac{\partial H}{\partial R_n} = -m\omega_0^2 R_n + \frac{1}{2}m\omega_1^2(R_{n+1} + R_{n-1}) + 4U_0\frac{1}{R_0^2}\left[1 - \left(\frac{R_n}{R_0}\right)^2\right]R_n$$
$$-m\chi_1(u_{n+1} - u_{n-1})R_n - m\chi_2[(u_{n+1} - u_n)R_{n+1} - (u_n - u_{n-1})R_{n-1}] \qquad (6)$$

$$\dot{P}_n = -\frac{\partial H}{\partial u_n} = \beta(u_{n+1} + u_{n-1} - 2u_n) + \frac{1}{2}m\chi_2(R_{n+1}^2 - R_{n-1}^2) + m\chi_2(R_n R_{n+1} - R_n R_{n-1}). \quad (7)$$

In the continuum approximation with the long-wavelength limit we have

$$nu_0 \to x \qquad \sum_n \to \frac{1}{u_0}\int \mathrm{d}x$$

with

$$R_{n\pm1} = R_n \pm u_0\frac{\partial R_n}{\partial x} + \frac{1}{2}u_0^2\frac{\partial^2 R_n}{\partial x^2} + \cdots \qquad R_n(t) \to R(x,t)$$

and

$$u_{n\pm1} = u_n \pm u_0\frac{\partial u_n}{\partial x} + \frac{1}{2}u_0^2\frac{\partial^2 u_n}{\partial x^2} + \cdots \qquad u_n(t) \to u(x,t)$$

and obtain

$$\frac{\partial^2}{\partial t^2}R(x,t) = \frac{1}{2}\omega_1^2 u_0^2\frac{\partial^2}{\partial x^2}R(x,t) + (\omega_1^2 - \omega_0^2)R(x,t) + \frac{4}{m}U_0 R_0^{-2}\left[1 - \left(\frac{R(x,t)}{R_0}\right)^2\right]R(x,t)$$
$$-2(\chi_1 + \chi_2)u_0\frac{\partial u(x,t)}{\partial x}R(x,t) \quad (8)$$

and

$$\frac{\partial^2}{\partial t^2}u(x,t) = C_0^2\frac{\partial^2}{\partial x^2}u(x,t) + (\chi_1 + \chi_2)mu_0\frac{1}{M}\frac{\partial}{\partial x}R^2(x,t). \quad (9)$$

We now set $\rho = x - vt$ and obtain from (9)

$$\frac{\partial}{\partial x}u(x,t) = -\frac{mu_0(\chi_1 + \chi_2)}{MC_0^2(1 - s^2)}R^2(x,t) + g \quad (10)$$

where g is an, as yet, undetermined integration constant and $s = v/C_0$. Substituting (10) into (8) we obtain

$$\frac{\partial^2}{\partial t^2}R(x,t) - v_1^2\frac{\partial^2}{\partial x^2}R(x,t) - [\omega_1^2 - \omega_0^2 + 2gu_0(\chi_1 + \chi_2)]R(x,t)$$
$$-\frac{4U_0}{mR_0^4}[R_0^2 - R^2(x,t)]R(x,t) - \frac{2(\chi_1 + \chi_2)^2 mu_0^2}{MC_0^2(1 - s^2)}R^3(x,t) = 0 \quad (11)$$

where $v_1^2 = \frac{1}{2}\omega_1^2 u_0^2$. We see from (11) that the interaction between protons and heavy ions indeed results in the decrease of the height of the barrier of the double-well potential. This helps the transfer of protons across the barrier in hydrogen-bonded systems. If we further set

$$\epsilon = \omega_1^2 - \omega_0^2 + \frac{4U_0}{mR_0^2} - 2g(\chi_1 + \chi_2)u_0 \qquad G = \frac{4U_0}{mR_0^4} - \frac{2(\chi_1 + \chi_2)^2 mu_0^2}{MC_0^2(1 - s^2)}$$

(11) becomes

$$R_{tt}(x,t) - v_1^2 R_{xx}(x,t) - \epsilon R(x,t) + GR^2(x,t)R(x,t) = 0. \quad (12)$$

Equation (12) is a standard ϕ^4 equation [43]. We assume a solution of the form

$$R(x,t) = F(\rho) \qquad \rho = x - vt \quad (13)$$

where k, ω and v are constants. Inserting (13) into (12) we get

$$(v^2 - v_1^2)\left(\frac{\mathrm{d}F}{\mathrm{d}\rho}\right)^2 - \varepsilon F^2 + \frac{1}{2}GF^4 = g'. \quad (14)$$

Here we choose the integration constant $g' = -\varepsilon^2/2G$.

We now consider in detail the solutions of (14).

(1) When $\epsilon > 0$, $G > 0$

$$\frac{4}{mR_0^4}\left(U_0 - \frac{(\chi_1+\chi_2)^2 m^2 u_0^2 R_0^4}{2MC_0^2(1-s^2)}\right) > 0$$

$$\omega_1^2 - \omega_0^2 + \frac{4U_0}{mR_0^2} - 2g(\chi_1+\chi_2)u_0 > 0 \tag{15}$$

and

$$0 < v < v_1 \qquad 0 < v < C_0. \tag{16}$$

These conditions imply that in the case of the protons the double-well potential dominates over the coupling interaction, i.e. the properties of the protons are mainly determined by the double-well potential in such a case. The soliton solution then has the form

$$F(\rho) = \pm\left(\frac{\varepsilon}{G}\right)^{1/2} \tanh\left[\left(\frac{\varepsilon}{2(v_1^2-v^2)}\right)^{1/2}\rho\right] \tag{17}$$

or

$$R(x,t) = \pm\left(\frac{\varepsilon}{G}\right)^{1/2} \tanh\left[\left(\frac{\varepsilon}{2(v_1^2-v^2)}\right)^{1/2}(x-vt)\right]. \tag{18}$$

This is a topological kink soliton. From (10) and (18) we obtain (writing $u_x(x,t) = \partial u/\partial x$ and similarly $u_t(x,t)$ later)

$$u_x(x,t) = \frac{(\chi_1+\chi_2)mu_0\varepsilon}{MC_0^2(1-s^2)G}\cosh^{-2}\left[\left(\frac{\varepsilon}{2(v_1^2-v^2)}\right)^{1/2}(x-vt)\right] \tag{19}$$

and

$$u(x,t) = \mp\frac{\sqrt{2}(\chi_1+\chi_2)mu_0}{MC_0^2(1-s^2)G}[\varepsilon(v_1^2-v^2)]^{1/2}\tanh\left[\left(\frac{\varepsilon}{2(v_1^2-v^2)}\right)^{1/2}(x-vt)\right]. \tag{20}$$

Here we choose

$$g = \frac{R_0^2 mu_0(\chi_1+\chi_2)}{MC_0^2(1-s^2)}.$$

Obviously the expression (20) is also a kink solution.

(2) When $0 < v < C_0$, $0 < v_1 < v$ and $\epsilon < 0$, $G < 0$ we have

$$\omega_0^2 - \omega_1^2 + 2g(\chi_1+\chi_2)u_0 - \frac{4U_0}{mR_0^2} > 0 \tag{21}$$

and

$$\frac{4}{mR_0^4}\left(\frac{m^2u_0^2(\chi_1+\chi_2)^2R_0^4}{2MC_0^2(1-s^2)} - U_0\right) > 0. \tag{22}$$

These conditions imply that the coupling of protons and heavy ions is more important than the double-well potential, i.e. the properties of the protons are predominantly determined by the coupling interaction. The solutions of (12) still have the form of (18)–(20).

(3) If $0 < C_0 < v$, we have

$$G = -\frac{4}{mR_0^4}\left(\frac{m^2u_0^2R_0^4(\chi_1+\chi_2)^2}{2MC_0^2(s^2-1)} + U_0\right) < 0. \tag{23}$$

Then the solution retains the soliton form of (18)–(20) if $0 < v_1 < 0$ and $\epsilon < 0$, i.e.

$$\omega_0^2 - \omega_1^2 + 2g(\chi_1+\chi_2)u_0 - \frac{4U_0}{mR_0^2} > 0. \tag{24}$$

The schematic form of the soliton solutions of (18)–(20) for $R(x,t) > 0$ are shown in figure 7.

(4) If $\epsilon < 0$, $G < 0$, i.e.

$$\omega_0^2 - \omega_1^2 - \frac{4U_0}{mR_0^2} > 0 \qquad \frac{4}{mR_0^4}\left(\frac{(\chi_1+\chi_2)^2 m^2 u_0^2 R_0^4}{2MC_0^2(1-s^2)} - U_0\right) > 0 \tag{25}$$

and

$$0 < v < C_0 \qquad 0 < v < v_1 \tag{26}$$

the soliton solution of (12) is of the form

$$F(\rho) = \pm\left[\frac{2|\varepsilon|}{|G|}\right]^{1/2} \cosh^{-1}\left[\left(\frac{|\varepsilon|}{v_1^2 - v^2}\right)^{1/2}\rho\right]$$

so that

$$R(x,t) = \pm\left[\frac{2|\varepsilon|}{|G|}\right]^{1/2} \cosh^{-1}\left[\left(\frac{|\varepsilon|}{v_1^2 - v^2}\right)^{1/2}(x - vt)\right]. \tag{27}$$

This expression represents a non-topological soliton or bounce. From (10) and (27) we obtain

$$u_x = -\frac{2mu_0(\chi_1+\chi_2)|\varepsilon|}{MC_0^2(1-s^2)|G|} \cosh^{-2}\left[\left(\frac{|\varepsilon|}{v_1^2 - v^2}\right)^{1/2}(x - vt)\right]$$

and

$$u(x,t) = \mp\frac{2(\chi_1+\chi_2)mu_0[|\varepsilon|(v_1^2 - v^2)]^{1/2}}{MC_0^2(1-s^2)|G|} \tanh\left[\left(\frac{|\epsilon|}{v_1^2 - v^2}\right)^{1/2}(x - vt)\right]. \tag{28}$$

The latter is again a topological kink solution. It may be noticed that we choose the integration constant g to be zero in accordance with the boundary conditions of $R(x,t)$ and $u(x,t)$. Therefore the difference between the two types of solutions results here from the boundary conditions.

(5) However, if we let

$$0 < v < C_0 \qquad 0 < v_1 < v \tag{29}$$

and $\epsilon > 0$, $G > 0$, we have

$$\omega_1^2 - \omega_0^2 + \frac{4U_0}{mR_0^2} > 0$$
$$\frac{4}{mR_0^4}\left(U_0 - \frac{(\chi_1+\chi_2)m^2u_0^2R_0^4}{2MC_0^2(1-s^2)}\right) > 0 \tag{30}$$

the solutions of (12) still have the form of (27) and (28).

(6) If we let $0 < C_0 < v$, then

$$G = -\frac{4}{mR_0^4}\left(\frac{m^2u_0^2R_0^4(\chi_1+\chi_2)^2}{2MC_0^2(1-s^2)} + U_0\right) < 0. \tag{31}$$

Thus only if $0 < v < v_1$, $\epsilon < 0$ the solutions of (12) can have the form of those of (27) and (28).

4. Elementary properties of proton solitons

We now investigate the elementary properties of the above proton solitons, but here we consider only a few physically important quantities concerning the kink and antikink solitons in (18)–(20).

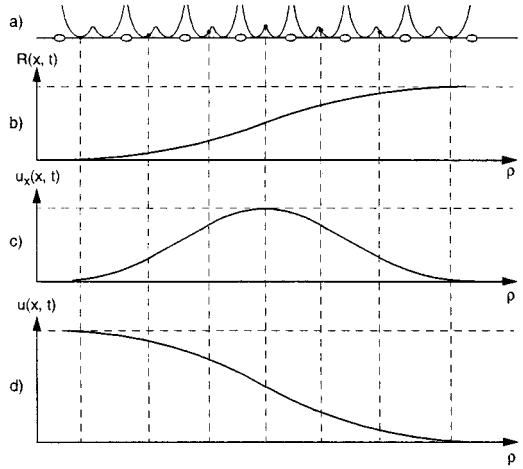

Figure 7. Schematic form of the solitons of (18)–(20).

4.1. Energy and mass of the soliton

When one soliton of either type is present in the chain the continuum expression of the energy corresponding to (12) becomes (R_x and R_t, again being partial derivatives)

$$E = \int_{-\infty}^{\infty} H\,\mathrm{d}x = \frac{1}{u_0}\int_{-\infty}^{\infty} m\left(\frac{1}{2}R_t^2 + \frac{1}{2}v_1^2R_x^2 - \frac{1}{2}\epsilon R^2 + \frac{G}{4}R^4\right)\mathrm{d}x. \tag{32}$$

Here the first term is the kinetic energy, the second term contains the (elastic) linear interaction and the remaining part is the potential of the model. Thus the energy of the soliton of (18) is

$$E = \frac{m\varepsilon}{2G}\left\{-\varepsilon\left[1 - \frac{1}{u_0}\left(\frac{2(v_1^2 - v^2)}{\varepsilon}\right)^{1/2}\right] + \varepsilon\left[\frac{1}{2} - \frac{2}{3u_0}\left(\frac{\varepsilon}{2(v_1^2 - v^2)}\right)^{-1/2}\right] + \frac{2}{3u_0}\left(\frac{\varepsilon}{2(v_1^2 - v^2)}\right)^{1/2}(v^2 + v_1^2)\right\}. \tag{33}$$

This energy of the soliton is related to the velocity of the soliton. Its dependence on the velocity in the case of ice is shown in figure 8. In this diagram we choose the following acceptable values of the parameters of the model (cf [1–37]): $R_0 = 1$ Å, $U_0 = 10$ eV, $M = 100m_p$, $m = m_p$, $v_1 = 10^3$ m s^{-1}, $C_0 = 10^4$ m s^{-1}, $u_0 = 5$ Å, $\chi_1 = 3 \times 10^{47}$ m s^{-2}, $\chi_2 = 0.2 \times 10^{44}$ m s^{-2}. Very obviously the energy increases with an increase in the velocity of the soliton. In figure 9 we plot the energy of the soliton against the sum of the coupling coefficients $\chi_1 + \chi_2$. It is seen that when this quantity increases, the energy of the soliton also increases. When the velocity of the soliton is very small, its energy of can be written

$$E_{sol} = E_0 + \tfrac{1}{2}M_{sol}v^2 \tag{34}$$

where

$$E_0 = \frac{m\varepsilon}{2G}\left\{-\varepsilon\left[1 - \frac{1}{u_0}\left(\frac{2v_1}{\varepsilon}\right)^{1/2}\right] + \varepsilon\left[\frac{1}{2} - \frac{2}{3u_0}\left(\frac{2v_1}{\varepsilon}\right)^{-1/2}\right] + \frac{2v_1}{3u_0}\left(\frac{\varepsilon}{2}\right)^{1/2}\right\} \tag{35}$$

is the rest energy of the soliton in this case. The relationship between the energy and the velocity is similar to that in the classical theory, where the mass of the soliton is taken to be

$$M_{sol} = \frac{m(\varepsilon)^{3/2}}{u_0}\left\{\sqrt{2}v_1\left[\frac{4U_0}{mR_0^4} - \frac{2(\chi_1 + \chi_2)^2 mu_0^2}{MC_0^2}\right]\right\}^{-1} = \text{constant}. \tag{36}$$

The soliton mass is also seen to increase with increasing coupling strength.

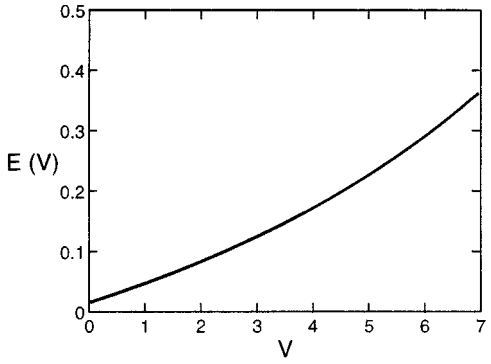

Figure 8. The dependence of the energy of the soliton on the soliton velocity.

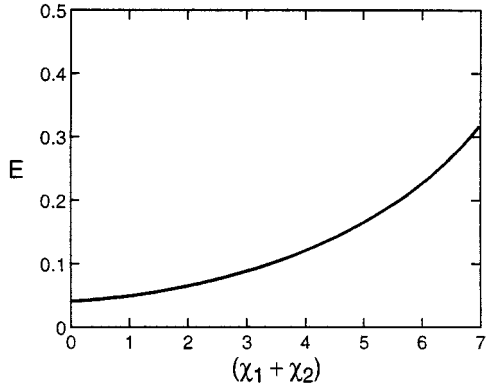

Figure 9. The dependence of the energy of the soliton on the coupling constants $\chi_1 + \chi_2$.

4.2. The momentum of the soliton

One can obtain the momentum P of the soliton from

$$P = -\frac{m}{u_0}\int R_x R_t \,\mathrm{d}x.$$

Inserting (18) we obtain $P = m^* v$ where

$$m^* = \frac{2\sqrt{2}m}{3u_0(v_1^2 - v^2)^{1/2}}\left(\frac{4U_0}{mR_0^4} - \frac{2(\chi_1+\chi_2)^2 u_0^2 m}{MC_0^2(1-s^2)}\right)^{-1}\varepsilon^{3/2} \tag{37}$$

and m^* is the effective mass of the soliton. Evidently the momentum of the effective mass of the soliton increases with increasing soliton velocity.

4.3. Amplitude and width of the soliton

The amplitude of the soliton of (18) is

$$R_m = \left[2\left(\omega_1^2 - \omega_0^2 + \frac{4U_0}{mR_0^2} - 2g(\chi_1+\chi_2)u_0\right)\left(\frac{4U_0}{mR_0^4} - \frac{2(\chi_1+\chi_2)^2 m u_0^2}{MC_0^2(1-s^2)}\right)^{-1}\right]^{1/2}.$$

Obviously R_m increases with increasing soliton velocity, but its dependence on the coupling constants $\chi_1 + \chi_2$ is weak. However, since the height of the barrier of the double-well potential

decreases with an increase in the coupling constants, in this case the soliton can more easily cross the barrier for proton transfer. The width of the soliton is

$$W_k = \pi u_0 \left(\frac{v_1^2 - v^2}{\omega_1^2 - \omega_0^2 + (4U_0/mR_0^2) - 2gu_0(\chi_1 + \chi_2)} \right)^{1/2}. \tag{38}$$

We see that the width of the soliton decreases as the coupling decreases and the soliton velocity v increases. However, the soliton width is regulated by the relative magnitude of the height of the barrier and that of the coupling constants.

4.4. The kink–antikink soliton pairs

We see from (18)–(20) that if the nonlinear autolocalized excitation in the protonic sublattice is a kink (or antikink) there is also an antikink (or kink) soliton in the heavy ionic sublattice, which is a 'shadow' of the kink (or antikink). They propagate along the hydrogen-bonded chains in pairs with the same velocity, as shown in figure 10. In this figure the curve 1(3) corresponds to the kink soliton in the protonic sublattice and curve 2(4) corresponds to the antikink soliton in the heavy ionic sublattice. The motion of the kink soliton pair results in some special physical and biological phenomena, which will be discussed in a separate paper. From (18)–(20) and the appropriate boundary conditions we find the momentum of the kink pair to be

$$P = -\frac{1}{u_0} \int (mR_x R_t + Mu_x u_t)\, \mathrm{d}x = P_k + P_{ak} = M_{sol}^* v \tag{39}$$

where P_k is the momentum of the protonic kink soliton of (18), and

$$P_{ak} = \frac{M}{u_0} \int u_x u_t \, \mathrm{d}x = M^* v$$

is the momentum of the antikink. Here $M_{sol}^* = m^* + M^*$ with

$$M^* \approx \frac{2\sqrt{2} M Q^2 h^{3/2}}{3u_0 b}$$

where

$$h = \left(\frac{U_0}{R_0^4} - \frac{2(\chi_1 + \chi_2)^2 u_0^2 m^2}{MC_0^2(1 - s^2)} \right) [m(v_1^2 - v^2)]^{-1}$$

and

$$b = \frac{G}{v_1^2 - v^2} \qquad Q = \frac{(\chi_1 + \chi_2) m u_0}{MC_0^2(1 - s^2)} \qquad m^* \approx \frac{2\sqrt{2} m h^{3/2}}{3u_0 b}$$

where m^* and M^* are the effective masses of the kink soliton and the antikink soliton respectively.

5. The potential of the system

It can be observed that (12) can be derived from the following effective Hamiltonian

$$H = \int m \left(\frac{1}{2} R_t^2 + \frac{1}{2} R_x^2 + U(R) \right) \mathrm{d}x \tag{40}$$

where the effective potential $U(R)$ is in such a case defined as

$$U(R) = -\tfrac{1}{2} m \epsilon R^2 - \tfrac{1}{4} G m R^4 + U_0. \tag{41}$$

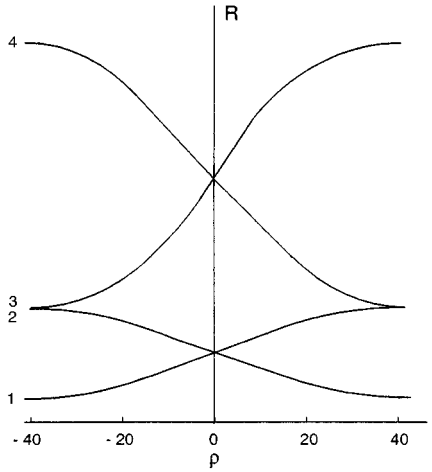

Figure 10. Kink–antikink soliton pairs in the hydrogen-bonded system.

The first term of (40) denotes the kinetic energy, the second term holds for the linear interaction and the third term is the potential with the R^4 type of interaction. On looking for solutions with a constant profile and moving at constant phase velocity v, which is a function of the variable $\rho = x - vt$, the Hamiltonian formulation yields the first integral of the motion, i.e.

$$\tfrac{1}{2}(v^2 - 1)(R_\rho^2) = U - U_0 \tag{42}$$

where U_0 is a constant of integration, i.e. the height of the barrier of the double-well potential. Equation (41) plays an important part in the existence and stability of the localized soliton solutions described above. The shape of the potential, equation (41), of course depends on the magnitudes of G and ϵ. Therefore the following several situations can be distinguished.

5.1. The case $\epsilon > 0$ and $G > 0$

This case implies that the double-well potential plays a main role for determining the properties of the protons, but the coupling interaction is only of secondary importance. This means that the double-well potential of (3) can make the protons become the kink solitons to cross over the barriers. Thus it also determines the properties of the soliton. The coupling interaction plays the role of reducing the height of the barrier, i.e. it contributes only a minor influence on the properties of the soliton. This point can be easily understood. In such a situation the potential has two degenerate minima with

$$U_{min} = -\left(\frac{\epsilon^2 m}{4G}\right) + U_0 = -\frac{m}{4}\left[\left(\omega_1^2 - \omega_0^2 + \frac{4U_0}{mR_0^4} - 2g(\chi_1 + \chi_2)u_0\right)^2 \times \left(\frac{4U_0}{mR_0^4} - \frac{2(\chi_1 + \chi_2)^2 m u_0^2}{MC_0^2(1 - s^2)}\right)^{-1}\right] + U_0 \tag{43}$$

at

$$\bar{R}_0 = R_{min} = \pm\left(\frac{\epsilon}{G}\right)^{1/2} = \pm\left\{\left(\omega_1^2 - \omega_0^2 + \frac{4U_0}{mR_0^2} - 2g(\chi_1 + \chi_2)u_0\right) \times \left(\frac{4U_0}{mR_0^4} - \frac{2(\chi_1 + \chi_2)^2 m u_0^2}{MC_0^2(1 - s^2)}\right)^{-1}\right\}^{1/2}. \tag{44}$$

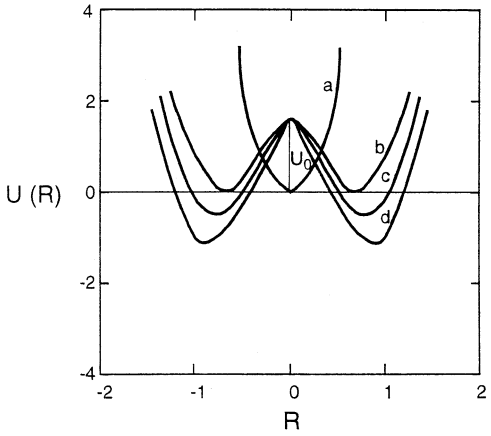

Figure 11. The potential energy $U(R)$ against R for different values of ϵ and G. Here we choose $m = 1$, $\epsilon > 0$ and $G > 0$. For curve (a) $\epsilon > 0$ and $G < 0$ or $\epsilon < 0$ and $G > 0$; curve (b) $\epsilon = \epsilon_0$ and $G = G_0$; curve (c) $\epsilon = 2\epsilon_0$ and $G = 1.5G_0$ and curve (d) $\epsilon = 3\epsilon_0$ and $G = 1.5G_0$. Here $G_0 > 0$, $\epsilon_0 > 0$ and let $\epsilon_0/G_0 = 1$.

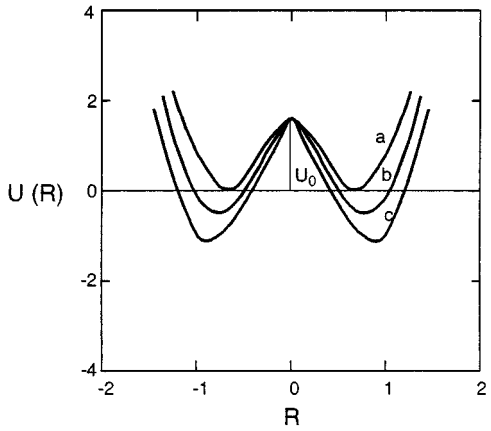

Figure 12. The potential energy of the system: $U(R)$ against R for different values of the coupling constants and $\epsilon > 0$ and $G > 0$. Here we choose $m = 1$. For curve (a) $\chi_1 + \chi_2 = 0$, curve (b) $\chi_1 + \chi_2 = 2$ and curve (c) $\chi_1 + \chi_2 = 4$.

Therefore the energy, $\bar{U}_{min}$, and the kink's position, $\bar{R}_0$, and the height of the barrier, $\bar{U}_0^*$, depend directly on the magnitudes of G/ϵ, or, put differently, on $(\chi_1 + \chi_2)$, ω_0, ω_1, v and U_0. When $\chi_1 = \chi_2 = 0$ and $\omega_1 = \omega_0 = 0$, we have $U_{min} = 0$ and $R = R_0$. This is just the case of the original double-well potential. However, if $\chi_1 \neq 0$, $\chi_2 \neq 0$, $\omega_0 \neq 0$ and $\omega_1 \neq 0$ the situation becomes very complicated. In figure 11 we plot $U(R)$ against R for different values of G and ϵ. Obviously the potential energy behaves quite differently in the cases of $\epsilon/G > 1.5$, $\epsilon/G < 1.5$ and $\epsilon/G = 1$. The heights of the barriers, $\bar{U}_0^*$, and the positions of the minima of the potential wells, $\bar{R}_0$, increase with the increase of ϵ and the decrease of G. The dependence of $U(R)$ on R in the case of different coupling constants $(\chi_1 + \chi_2)$ is shown in figure 12. We see from this figure that with an increase of the coupling constants the height of the barrier decreases and the positions of the minima of the potential wells are lengthened relative to the heavy ions. This means that for protons the possibility of transitions over the

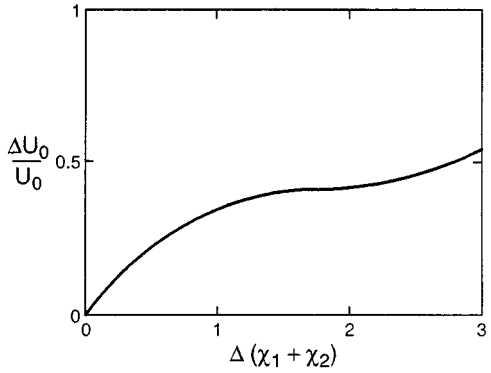

Figure 13. The dependence of the relative change of the height of the potential barrier on the change of the coupling constants for $\epsilon > 0$ and $G > 0$.

barrier is enhanced with an increase of the coupling constants. A decrease in the height of the barrier, $\bar{U}_0^*$, and the reduction of the equilibrium position, $\bar{R}_0$, are approximately given by

$$\Delta U_0 = U_0 - U_0[1 - (2z - z^2)(y + 1) + y] = U_0[(2z - z^2)(y + 1) - y] > 0 \tag{45}$$

with

$$\Delta \bar{R}_0 = R_0 - R_0\left(1 - \frac{z}{2}\right)\left(1 + \frac{y}{2}\right) = R_0\left[\frac{z}{2}\left(1 + \frac{y}{2}\right) - \frac{y}{2}\right] > 0 \tag{46}$$

where

$$0 < z = \frac{\omega_0^2 - \omega_1^2 + 2g(\chi_1 + \chi_2)u_0}{(4U_0/mR_0^2)}$$

$$0 < y = \frac{2(\chi_1 + \chi_2)m^2u_0^2R_0^4}{4U_0MC_0^2(1 - s^2)}$$

and

$$g = \frac{R_0^2mu_0(\chi_1 + \chi_2)}{MC_0^2(1 - s^2)} \qquad z > y.$$

Equations (45) and (46) clearly show that ΔU_0 and $\Delta \bar{R}_0$ increase with an increase in the coupling constants $(\chi_1 + \chi_2)$. In figure 13 we plot ΔU_0 against $(\chi_1 + \chi_2)$. At the same time, in this case, the values of the minima of the potential also become negative at $\bar{R}_0 < R$, from zero at $R = R_0$. The larger $(\chi_1 + \chi_2)$, the smaller $\bar{R}_0$, the lower the height of the barrier and the more negative the values of the minima of the potential energy. Thus the possibility of the protons jumping over the barriers is greatly enhanced. This clearly shows that the case of $\epsilon > 0$ and $G > 0$ describes the motion of the proton over the barrier of the double-well potential in intrabonds. Thus, the ionic defects occur in such a case in the hydrogen-bonded systems.

Also, above the minima of the potential energy, U_{min}, its position $\bar{R}_0$ decreases also with increasing of velocity of the proton. This shows that when the velocity of the protons is increased the protons will be far from the heavy ions. This conclusion has important consequences.

5.2. The case of $\epsilon < 0$ and $G < 0$

Contrary to the above situation, this means that the coupling interaction between the protons and the heavy ions plays the main and elementary role for determining the properties of the

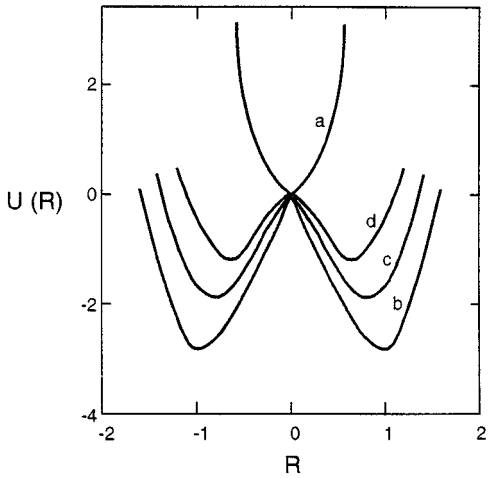

Figure 14. The dependence of the potential energy of the system on R for $\epsilon < 0$ and $G < 0$ for different values of ϵ' and G'. Here the origin of coordinates are at $R = \upsilon_0/2$ and the cases shown have: curve (a) $\epsilon > 0$ and $G < 0$ or $\epsilon < 0$ and $G > 0$; curve (b) $G' > g'_0$ and $\epsilon' < \epsilon'_0$; curve (c) $G' = G'_0$ and $\epsilon' = \epsilon'_0$; curve (d) $G' < G'_0$ and $\epsilon' > \epsilon'_0$. Here $G'_0 > 0$, $\epsilon'_0 > 0$, $\epsilon' = -\epsilon$, $G' = -G$, let $\epsilon'_0/G'_0 = 1$ and $m = 1$.

protons. In such a case, the coupling interaction makes the protons become the solitons to shift over the barriers in the interbonds, the double-well potential playing only a minor role. However, the potential of the system is still twofold degenerate and its minima or perturbation theory vacuum energies are

$$U'_{min} = \frac{m}{4}\frac{|\epsilon|^2}{|G|} - U_0 = \frac{m}{4}|\bar{R}'_0|^2|\epsilon| - U_0 < 0 \tag{47}$$

i.e. it is negative, with the positions

$$\bar{R}'_0 = \pm\left(\frac{|\epsilon|}{|G|}\right)^{1/2} = \pm\left(\frac{\epsilon'}{G'}\right)^{1/2} \qquad \epsilon' = -\epsilon, G' = -G. \tag{48}$$

In figure 14 we plot $U(R)$ against R for different values of G and ϵ. From this plot, (47) and (48) we see that when ϵ is small and G is large, $\bar{R}'_0$ is large and U_{min} is small and *vice versa*. Obviously U'_{min} and $\bar{R}'_0$ also depend on the coupling constants $(\chi_1 + \chi_2)$. In figure 15 we plot $\bar{R}'_0/R_0$ against the change of $(\chi_1 + \chi_2)$. The relations between these are approximately given by

$$\begin{aligned} &\bar{R}'_0 = \pm R_0(1 - \tfrac{1}{2}z')(1 + \tfrac{1}{2}y') \\ &z' = \frac{\omega_1^2 - \omega_0^2 + (4U_0/mR_0^2)}{2g(\chi_1 + \chi_2)} < 1 \qquad \frac{1}{y'} = y < 1 \end{aligned} \tag{49}$$

and

$$U'_{min} = \frac{mR_0^4}{4}\left(\frac{2(\chi_1 + \chi_2)mu_0^2}{MC_0^2(1 - s^2)}\right)(1 - z')^2(1 + y') - U_0 \qquad 0 < z',\ 0 < y',\ y' > z'. \tag{50}$$

We clearly see from figure 15 and (49) that when $(\chi_1 + \chi_2)$ increases then $\bar{R}'_0$ increases. This shows that strong coupling makes the protons approach the heavy ions, so that their separation changes considerably. Conversely, $\bar{R}'_0$ decreases when $(\chi_1 + \chi_2)$ decreases. This means that with increasing separation of the protons from the heavy ions, the coupling interaction between

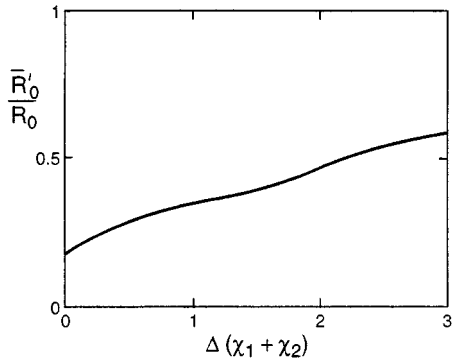

Figure 15. The relative values of equilibrium positions $\bar{R}_0'/R_0$ against the change of the coupling constants $\Delta(\chi_1 + \chi_2)$ for $\epsilon < 0$ and $G < 0$.

them also decreases. This is reasonable. Because there are two new equilibrium positions in such a case, the proton can shift to another side of a heavy ion owing to the way the velocity of the proton effects the potential energy of the system. Thus the rotation of the bonds, or Bjerrum defect, occurs in such a case in the system. Also, above the minima of the potential energy, U_{min} and $\bar{R}_0'$ increase with the velocity of the proton transfer and *vice versa*. This shows that the equilibrium positions are reduced relative to the heavy ions, when the protons approach the heavy ions at a high velocity; and *vice versa*, when the velocity of the proton decrease the protons will be far away from the ions, which is an important point.

5.3. The case $G > 0$ and $\epsilon < 0$ or $G < 0$ and $\epsilon > 0$

In such a case there is no double-well potential. There is only one minimum of the potential $U(R)$ in (41), i.e. $U_{min}(R) = 0$ at $R = 0$. The corresponding behaviour of the potential is shown in case (a) of figures 10 and 13. No localized soliton solution exists in this case.

6. Discussion and conclusions

We now discuss in detail the properties of the solitons obtained above and compare our results with those of previous models, explaining the advantages and the validity of this model.

(1) We first of all discuss the peculiarities of this model and its relation to proton transfer. It is well known that, in ice, as well as in water, after the protons have been transferred from one water molecule to another along the hydrogen bonded chains (as shown in figure 2), the chain is restored to its original state by the so-called Bjerrum defect (as shown in figure 3). This clearly shows that there are two distinct types of mechanisms of proton transfer in the hydrogen-bonded systems. However, there is one open problem in previous models, including the ADZ model and other generalizing models, which is how do the two types of defects can combine automatically and alternate spontaneously in the transfer process? Thus, how can we theoretically describe the mutually alternating transfer of the two types of defects? It is these problems that may be solved by the present model. In this model we utilize a unified idea to understand the proton transfer, i.e. whether the ionic defect or Bjerrum defect is produced by the changes of the relative positions of the protons and heavy ions under the action of an intrinsic nonlinear interaction. What distinguishes them is the interaction and the way the changes of relative positions occur in this phenomenon. The ionic defect is mainly produced by the double-well potential through the mechanism of jumping over the barriers in

the manner of translation and crossover in the intrabonds, but the Bjerrum defect is caused by the nonlinear coupling interaction through the mechanism of quasi-self-trapping in the manner of the relative shift of positions of the two bodies in the interbonds as described in earlier sections. In the transfer process the protons cross over the barriers in the intrabonds in the form of kink solitons (which result in the ionic defect), and the shift over the barriers in the interbonds in another soliton form (which results in the Bjerrum defect). The reason for this change is that the coupling interaction between the protons and the heavy ions changes with the change of the relative positions between them. When the protons cross the barriers in the intrabonds, the coupling interaction is small due to their long distance from the heavy ions, and so play a secondary part in determining the properties of the protons.

When the protons are near the heavy ions and cross over the barriers in the interbonds, the coupling interaction becomes so great that their positions relative to those of the heavy ions change considerably by means of the mechanism of quasi-self-trapping. In such a case the coupling interaction determines the principal properties of the protons, the latter transforming into another soliton form in the interbonds. However, the changes of the forms of the proton transfer are not sudden, but asymptotic. This point can be explained from the changes of the potential of the system with the change of coupling constants, $(\chi_1 + \chi_2)$, in (43), (44), (47) and (48). As a matter of fact, we see from (43) and (44) that the minima of the potential energy become more and more negative with increasing $(\chi_1 + \chi_2)$. When the latter become so great that their effect is greater than that of the double-well potential in (3), then the minimum of the potential energy of the system becomes just that of (47) and (48).

Therefore, the asymptotic changes of the potential energy of the system with the changes of the coupling interaction result in the asymptotic changes of the manners of the proton transfer or that of the proton soliton. Certainly, in this process the changes of the velocity of the proton transfer in different regions can also result in some changes of the potential energy of the system; thus it can also influence to some extent the form of the proton transfer as mentioned in section 5. This is due to the Hamiltonian in (1), in which we consider not only the double-well potential and the change of relative positions of neighbouring heavy ions resulting from the vibration or displacement of the protons, but also the electromagnetic interaction between the neighbouring protons and the resulting change in the relative positions of neighbouring heavy ions. Thus the protons can transfer in the form of two different types of solitons in the intrabonds and interbonds along the hydrogen-bonded chains through the competition between these two types of nonlinear interaction. This is a main advantage of our model. Also, it can give analytic solutions, which is a convenient property for analysing the properties of the proton solitons and the two types of defects.

(2) It is easy to elucidate the combined and alternate changes of the two types of defects if we consider the soliton solutions and their conditions, equations (15)–(31), and the properties of the potential energy of the system described in section 5. We see that when the conditions of (15) and (16) are satisfied, the defects occur, or—put differently—the excitation of the protons and the deformation of the heavy ionic sublattice generated in such a case are together transferred in the form of a kink–antikink soliton pair along the hydrogen-bonded chains. The physical meaning of this soliton with the plus sign in $R(x,t)$ in (18) is that the kink soliton results in a localized reduction of the protonic density (i.e. expansion of the proton sublattice) which amounts to creating a negatively charged carrier and an extended ionic defect moving with a velocity v less than the speed of sound C_0 and v_1 in the two sublattices. The above soliton solution corresponds to the OH^- ionic defect to appear in the Bernal–Fowler picture. The other soliton solution, with a minus sign in $R(x,t)$ in (18), represents the compression of the protonic sublattice and the increase of the localized proton density, which amounts to creating a positively charged carrier and an extended ionic defect. Therefore the latter

corresponds to the H_3O^+ ionic defect. Thus the two types of solutions in (18)–(20) represent the proton transfer in the form of ionic defects in the intrabonds accompanied by a localized deformation of the heavy ionic sublattice. This point has already been discussed in detail in section 5. However, the properties of the proton soliton in such a case are mainly determined by the double-well potential $U(R)$ since there is still the same type of soliton in the system if no coupling interaction is present. As a matter of fact when $\chi_1 = \chi_2 = 0$, (12) becomes

$$R_{tt} - v_1^2 R_{xx} - \epsilon_1 R + G_1 R^2 R = 0 \tag{51}$$

where $G_1 = 4U_0/mR_0^4 > 0$, $\epsilon_1 = \omega_1^2 - \omega_0^2 + (4U_0/mR_0^2) > 0$. Equation (51) has indeed soliton solutions with the same shape and properties as the soliton of (18); the only difference is that the amplitude and width of the soliton are slightly different. This clearly demonstrates the above point of view. Hence here we may refer to the above type of soliton as a KINK I soliton for convenience.

Contrary to the above KINK I soliton, the kink soliton arising with the conditions (21) and (22) is of the form

$$R(x,t) = \pm\left(\frac{\varepsilon'}{G'}\right)^{1/2} \tanh\left[\left(\frac{\varepsilon}{2(v^2 - v_1^2)}\right)^{1/2}(x - vt)\right] \tag{52}$$

where

$$G' = -G = \frac{4}{mR_0^4}\left(\frac{(\chi_1 + \chi_2)^2 m u_0^2 R_0^4}{2MC_0^2(1 - s^2)} - U_0\right) > 0$$
$$\epsilon' = -\epsilon = \omega_0^2 - \omega_1^2 + \left(\frac{2mu_0^2(\chi_1 + \chi_2)^2 R_0^2}{MC_1^2(1 - s^2)} - \frac{4U_0}{mR_0^2}\right) > 0. \tag{53}$$

Although the shape of this kink soliton, equation (52), is the same as that of (18), the essential features and properties of the soliton are vastly different from those of the soliton of (18). The properties of the soliton in (52) are mainly determined by the nonlinear coupling interaction between the protons and the heavy ions, because the kink soliton disappears if $\chi_1 = \chi_2 = 0$. Therefore the motion of the kink soliton cannot result in the above ionic defect, instead another type of defect occurs in the interbonds. Owing to the different properties of the soliton, and recalling again the corresponding properties of the potential energy of the system as discussed in section 5, we can see that it is the Bjerrum defect produced by the so-called rotation of the bond X–H arising from changes of the relative positions of the protons and the heavy ions in which an O–O bond with two protons and positive effective charge (the D Bjerrum defect) and one without proton and with negative effective charge (the L Bjerrum defect) occur. Therefore we may refer to this type of soliton as a KINK II. The plus sign of $R(x,t)$ in (53) applies to the L Bjerrum defect, which amounts to creation of a negative effective charge, and the minus sign in $R(x,t)$ in (53) applies in the case of the D Bjerrum defect which amounts to creation of a positive effective charge. Thus there really are two types of different defects in the hydrogen-bonded systems due to the localized fluctuations or displacements of the protons in this model. This may be summarized as:

$$\text{KINK I} \rightarrow I^- \text{ ionic defect}, \quad \text{KINK II} \rightarrow \text{L Bjerrum defect}$$

and

$$\text{anti-KINK I} \rightarrow I^+ \text{ ionic defect}, \quad \text{anti-KINK II} \rightarrow \text{D Bjerrum defect}.$$

Therefore with this model we can simultaneously describe the two types of defects which occur and their combined and internal transport in the hydrogen-bonded chains. This is a peculiarity of this model. As a matter of fact, the local coupling interaction between the two

sublattices introduced in the previous models, including the ADZ model and its generalizing models, does not allow consideration of multiple-defect dynamics. All two-component models can only support one pair of defects of each type, for example ionic defects. Pnevmatikos [15] also studied the propagation of the ionic and Bjerrum defects by using a double-sine interaction, but the mechanism of propagation is worth studying further; furthermore, his model does not give the detailed structure of alternate transport of the two types of defects.

(3) We now study the properties of the solitons shown in (27) and (28), which have not been obtained in previous models. It is well known that bounces are a kind of bell-shaped but non-topological solitons. This result shows that the protons can transfer along the hydrogen-bonded chains in the form of these bell-shaped solitary waves in the intrabonds and the interbonds with a constant velocity, less than the speed of sound, in the heavy ionic sublattice ($v < C_0$). In accordance with the viewpoint described above in points (1) and (2) of this section and the corresponding properties of the potential energy of the systems discussed in section 5 we can also arrive at the following conclusions. The two types of solitons determined by conditions (29) and (30) also describe the occurrence and motion of the I^- ionic defect with negative effective charge and the I^+ ionic defect with positive effective charge, respectively, when the protons cross the barrier from one molecule to another. The properties of this soliton are mainly determined by the double-well potential due to the conditions (29) and (30). However, the soliton given by (27) and (28) under the conditions of (25) and (26) or (31) has different properties. This shows the occurrence and transport of positive (D) and negative (L) Bjerrum defects generated by the rotations of the bonds, when the protons transfer in the interbonds along the hydrogen-bonded chains. In such a case the properties of the proton solitons are mainly determined by the nonlinear coupling interaction due to the conditions (25), (26) and (31). Therefore, these solitons determined by (25)–(31) can also describe the transport of the two types of defects which occur in hydrogen-bonded systems.

(4) From above results and (15)–(31) we see that the velocities of these solitons excited in the systems have a large domain including $v > (<)v_1$ and respectively $v < (>)C_1$, apart from $v = C_1$ and $v = v_1$. The extensive changes of velocity of the solitons are helpful to make the proton transfer match the changes of the potential energy of the systems, and thus make the protons easily cross over different barriers in the intrabonds and the interbonds as described in section 5. This is also an advantage of our model. As a matter of fact, analytical soliton solutions are supported in very small domains of velocity in the previous models, including the ADZ model, which has an analytic solution for one single constant value. The authors of [14] obtained numerical solutions with a perturbative method for a broader range of velocities in the domain $v_1 < v < v_0$. The lower bound of this domain is generally different from zero except for small coupling or a large ratio C_0/v_0. However, for physical reasons, taking into account the inertia of the oxygen sublattice in ice, the breakdown of their two-component solitary wave may be expected to occur at high velocities rather than at smaller velocities.

The response of the soliton in this model to an external field will be examined elsewhere, which is important for the determination of physical consequences of the soliton which can be tested experimentally, such as conductivity.

Acknowledgment

X-FP acknowledges support by a DAAD–KC Wong fellowship, and the National Natural Science Foundation of China grant No 19974034.

References

[1] Antonchenko V Ya, Davydov A S and Zolotaryuk A V 1983 *Phys. Status Solidi* b **115** 631
[2] Laedke E W, Spatschek K H, Wilkens M and Zolotaryuk A V 1985 *Phys. Rev.* A **32** 1161
[3] Nagle J F and Morowitz H J 1978 *Proc. Natl Acad. Sci. USA* **75** 298
[4] Nagle J F, Mille M and Morowitz H J 1980 *J. Chem. Phys.* **72** 3959
[5] Nagle J F and Nagle S T 1983 *J. Membr. Biol.* **74** 1
[6] Bernal J D and Fowler R H 1933 *J. Chem. Phys.* **1** 515
[7] Bjerrum N 1952 *Science* **115** 385
[8] Eigen M and De Maeyer L 1958 *Proc. R. Soc.* A **247** 505
[9] Onsager L 1973 *Physics and Chemistry of Ice* ed E Whalley, S J Jones and L W Crold (Ottawa: RSC) pp 7–12
[10] Sokolov N D 1955 *Usp. Fiz. Nauk.* **57** 205
[11] Sergienko A I 1988 *Sov. Phys.–Solid State* **30** 496
Sergienko A I 1987 *Phys. Status Solidi* b **144** 471
[12] Sergienko A I 1990 *Sov. Phys.–JETP* **70** 710
[13] Yomosa S 1982 *J. Phys. Soc. Japan* **51** 3318
[14] Peyrared M, Pnevmatikos St and Flytzanis N 1987 *Phys. Rev.* A **36** 903
[15] Pnevmatikos St 1988 *Phys. Rev. Lett.* **60** 1534
[16] Kristoforov L N and Zolotaryuk A V 1988 *Phys. Status Solidi* b **146** 487
[17] Pnevmatikos St, Flytzanis N and Bishop A R 1987 *J. Phys. C: Solid State Phys.* **20** 2829
[18] Kashimori Y, Kikuchi T and Nishimoto K 1982 *J. Chem. Phys.* **77** 1904
[19] Hochstrasser D, Buttner H, Desfontaines H and Peyrared M 1989 *J. Physique Coll.* **50** 3
[20] Chochliouros I and Pouget J 1995 *J. Phys.: Condens. Matter* **7** 8741
[21] Bontis T 1992 *Proton Transfers in Hydrogen Bonded Systems* (London: Plenum)
[22] Schuster P, Zundel G and Sandorfy C 1976 *The Hydrogen Bond, Recent Developments in Theory and Experiments* (Amsterdam: North Holland)
[23] Zdotaryuk A V, Spatschek R H and Ladre L E W 1984 *Phys. Lett.* A **101** 517
[24] Zdotaryuk A V 1986 *Theor. Math. Fiz.* **68** 415
[25] Peyrared M, Pnevmatikos St and Flytzanis N 1986 *Physica* D **19** 268
[26] Weberpals H and Spatschek K H 1987 *Phys. Rev.* A **36** 2946
[27] Hochstrasser D, Buttner H, Desfontaines H and Peyrared M 1988 *Phys. Rev.* A **38** 5332
[28] Desfontaines H and Peyrared M 1989 *Phys. Lett.* A **142** 128
[29] Halding J and Lomdahl P S 1988 *Phys. Rev.* A **37** 2608
[30] Braum J M and Klvshar Yu S 1990 *Phys. Lett.* A **149** 119
Braum J M and Klvshar Yu S 1991 *Phys. Rev.* B **43** 1060
Klivshar Yu S 1991 *Phys. Rev.* A **43** 3117
[31] Fraggs T, Pnevmatikos St and Economon E N 1989 *Phys. Lett.* A **142** 361
[32] Yomosa S 1982 *J. Phys. Soc. Japan* **51** 3310
Yomosa S 1983 *J. Phys. Soc. Japan* **52** 1866
[33] Marcheson F 1986 *Phys. Rev.* B **34** 6536
[34] Buttiker M and Ladauer R 1981 *Phys. Rev.* A **23** 1397
[35] Pnevmatikos St, Savin A V, Zolotaryuk A V, Kivshar Yu S and Velgakis M J 1991 *Phys. Rev.* A **43** 5518
[36] Zolotaryuk A V and Pnevmatikos St 1990 *Phys. Lett.* A **143** 233
Tsironis G P and Pnevmatikos St 1989 *Phys. Rev.* B **39** 7161
[37] Mei Y P, Yan J R, Yan X H and You J Q 1993 *Phys. Rev.* B **48** 575
Mei Y P and Yan J R 1993 *Phys. Lett.* A **180** 259
[38] Pang Xiao-feng 1990 *J. Phys.: Condens. Matter* **2** 9541
Pang Xiao-feng 1994 *Phys. Rev.* E **49** 4747
Pang Xiao-feng 1998 *Acta Phys. Slovak* **47** 217
[39] Pang Xiao-feng 1993 *Acta Phys. Sinica* **42** 1872
Pang Xiao-feng 1997 *Acta Phys. Sinica* **46** 625
[40] Pang Xiao-feng 1993 *Chinese Phys. Lett.* **10** 381
Pang Xiao-feng 1993 *Chinese Phys. Lett.* **10** 437
Pang Xiao-feng 1993 *Chinese Phys. Lett.* **10** 517
[41] Pang Xiao-feng 1993 *Chinese Sci. Bull.* **38** 1557
Pang Xiao-feng 1993 *Chinese Sci. Bull.* **38** 1665
[42] Pang Xiao-feng 1993 *Acta Math. Sci.* **13** 437
Pang Xiao-feng 1996 *Acta Math. Sci.* **16** 1
[43] Pang Xiao-feng 1994 *Theory of Non-linear Quantum Mechanics* (Chonqing: Chinese Chonqing)
Pang Xiao-feng 1999 *Eur. J. Phys.* B **10** 415